Int. J. Heat Mass Transfer. Vol. 15, pp. 2489–2498. Pergamon Press 1972. Printed in Great Britain

ROUGH ANNULUS PRESSURE DROP—INTERPRETATION OF EXPERIMENTS AND RECALCULATION FOR SQUARE RIBS

K. MAUBACH
Institut fur Neutronenphysik und Reaktortechnik, Kernforschungszentrum, 75 Karlsruhe 1, Postfach 3640, Germany

(*Received* 15 *December* 1971)

Abstract—A method is presented which allows the interpretation of pressure drop measurements with rough tubes, annuli and parallel plates. A parameter deduced describes the effect of roughness on a turbulent velocity profile. As a result, experimental data with various roughnesses and channel geometries can be generalized and made comparable. The paper summarizes the results of the interpretation of data with rectangular cross section roughnesses given by numerous authors in the literature.

Finally, examples of the recalculation of friction factors are shown, provided that Reynolds numbers of the flow, channel and roughness geometries are given. The results prove that the method proposed enables us to calculate friction factors of isothermal turbulent flow in concentric annuli with rough inner tubes with a precision which is sufficient for design problems.

NOMENCLATURE

Geometrical parameters

- x, coordinate in the direction of flow;
- y, coordinate perpendicular to the wetted wall;
- F, cross section of flow;
- P, wetted perimeter (τ_W);
- D, hydraulic diameter, $4F/P$;
- r, radius;
- α, β, γ, annular gap parameter, equations (3)–(5);
- s, h, b, distance, height, width, respectively, of roughness elements
- G, parameter of geometry, equations (12) and (13);
- y^+, dimensionless wall distance, $= y \cdot U^*/\nu$;
- h^+, dimensionless height of roughness, $= h \cdot U^*/\nu$.

Flow data

- p, pressure;
- ρ, density;
- ν, kinematical viscosity;
- λ, friction factor;
- τ, τ_W, shear stress, wall shear stress;
- U, local velocity;
- $\bar{U}$, average velocity;
- U^*, shear stress velocity, $\sqrt{(\tau_W/\rho)}$;
- U^+, dimensionless velocity, U/U^*,
- $R(h^+)$, roughness function;
- R, numerical values of roughness function for large h^+;
- K, constant.

INTRODUCTION

ARTIFICIAL roughness as a means of improving heat transfer gains more and more interest, especially for application to gas cooled reactors. The thermodynamic design of the reactor core calls for knowledge of the heat transfer data and pressure losses generated by roughnesses. Therefore, a considerable number of experimental investigations have been performed and will be performed in the future in order to find the most appropriate forms of roughness. For investigations involving a broad variation of the geometrical roughness parameters it will be

useful to work with a simple channel geometry which limits experimental costs. This resulted in the use of the concentric annular gap with rough inner tube in a large number of experiments. In the following paragraphs, turbulent flow in the concentric annular gap will be described and a method will be indicated which allows the interpretation of pressure loss measurements. In this way, general parameters can be derived from the experimental results which help to calculate the hydraulic behavior of the flow.

TURBULENT FLOW IN AN ANNULAR GAP WITH ROUGHENED INNER TUBE

The pressure loss of a flow in the annular gap is given by the following equation which defines the friction factor:

$$\frac{dp}{dx} = \lambda \frac{\rho}{2} \overline{U}^2 \frac{1}{D} \tag{1}$$

where D is the so-called "hydraulic diameter"

$$D = \frac{4F}{P} \tag{2}$$

If λ is known as a function of the Reynold's number, the channel form, and the geometrical form of roughness, the pressure loss can be calculated.

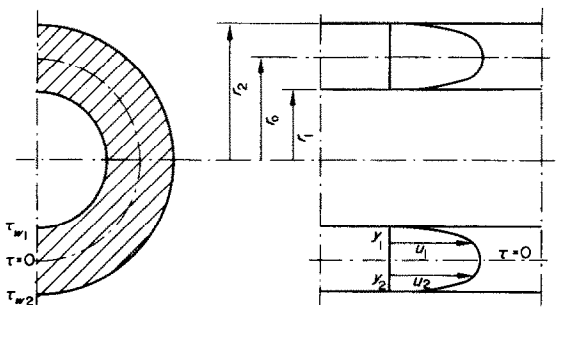

$\alpha = r_1/r_2$ $\beta = r_0/r_2$ $\gamma = r_0/r_1$

FIG. 1. Annulus separated in zones.

In the case of the concentric annular gap with roughened inner tube represented in Fig. 1, an additional difficulty is encountered in the interpretation of the experiments and calculation of the pressure loss. This difficulty is due to the interaction of the roughened inner and the smooth outer walls.

The difficulty mentioned above is overcome by the following assumption: Let the flow in the concentric annular gap by hydraulic like the flow in two fictitious annular zones which are combined in an appropriate manner [1].

Annular zones are the inner zone (Fig. 1), which is limited by the inner roughened wall, and the line with the shear stress $\tau = 0$, geometrically defined by

$$\gamma = r_0/r_1 \tag{3}$$

as well as the outer zone between the $\tau = 0$ line and the outer wall, characterized by

$$\beta = r_0/r_2. \tag{4}$$

If the annular gap is described by:

$$\alpha = r_1/r_2 \tag{5}$$

we obtain

$$\gamma = \beta/\alpha. \tag{6}$$

As shown in [1], the experimental results available justify the assumption that the universal laws of velocity distribution found for the circular tube are applicable also to these annular zones.

In the outer smooth zone (index 2) the velocity profile of the smooth tube (law of the wall) is applicable:

$$U_2^+ = 2{\cdot}5 \ln y_2^+ + 5{\cdot}5. \tag{7}$$

The following relation applies to the inner roughened zone (index 1)

$$U_1^+ = 2{\cdot}5 \ln \frac{y_1}{h} + R(h^+) \tag{8}$$

where $R(h^+)$ is determined by the form of the roughness elements (e.g. s/h and h/b for transversal ribs with rectangular cross sections).

Thus, the nature of the wall determines the form of the velocity profile. The friction factor is defined in addition by the form of the channel which determines the magnitude of the parameter

$$G = U_{max}^{+} - \bar{U}^{+} \tag{9}$$

which in turn is directly substituted in the friction law, as shown in [1].

The following friction laws can be derived:

Inner roughened zone:

$$\sqrt{\left(\frac{8}{\lambda_1}\right)} = 2{\cdot}5 \ln\left[\frac{r_0 - r_1}{h}\right] + R(h^+) - G_1(\gamma) \tag{10}$$

Outer smooth zone:

$$\sqrt{\left(\frac{8}{\lambda_2}\right)} = 2{\cdot}5 \ln\left[\frac{r_2 - r_0}{\nu} U_2^{+}\right] + 5{\cdot}5 - G_2(\beta). \tag{11}$$

It applies that

$$G_1(\gamma) = \frac{K \times 3{\cdot}75 + 1{\cdot}25 \times \gamma}{1 + \gamma} \tag{12}$$

$$G_2(\beta) = \frac{K \times 3{\cdot}75 + 1{\cdot}25 \times \beta}{1 + \beta}. \tag{13}$$

K constitutes an empirical parameter introduced as a means of fitting the experimental results; it takes the following numerical values [1]:

$K = 1{\cdot}0576$ for smooth zones; $K = 1$ for roughened zones.

The velocity profiles originating from the two walls intersect at the velocity U_{max} defined in Fig. 2:

It follows from (8) for U_{max} at the distance $r_0 - r_1$:

$$\frac{U_{max}}{U_1^*} = 2{\cdot}5 \ln \frac{r_0 - r_1}{h} + R(h^+) \tag{14}$$

and from (7):

$$\frac{U_{max}}{U_2^*} = 2{\cdot}5 \ln\left[\frac{r_2 - r_0}{\nu} U_2^*\right] + 5{\cdot}5. \tag{15}$$

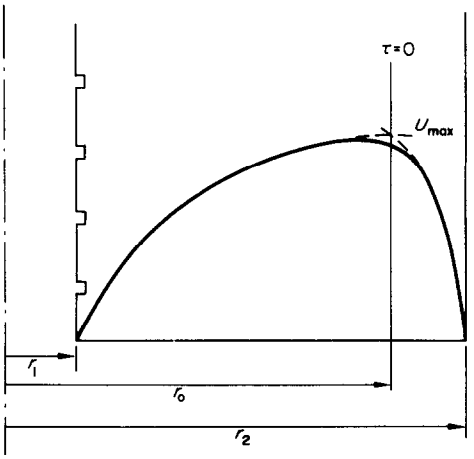

FIG. 2. Hypothetical velocity profiles in annuli.

After elimination of U_{max}, equations (14) and (15) yield:

$$\frac{U_1^*}{U_2^*} = \frac{2{\cdot}5 \ln\left[\frac{r_2 - r_0}{\nu} U_2^*\right] + 5{\cdot}5}{2{\cdot}5 \ln \frac{r_0 - r_1}{h} + R(h^+)}. \tag{16}$$

Another equation provides the condition of continuity:

$$\frac{\bar{U}_1}{\bar{U}} \frac{F_1}{F} + \frac{\bar{U}_2}{\bar{U}} \frac{F_2}{F} = 1. \tag{17}$$

These equations are employed to determine the required friction factor. This calls for a number of transformations which are described below.

A comparison of forces gives for the mean wall shear stress:

$$\bar{\tau}_W = \frac{dp}{dx} \cdot \frac{D}{4}. \tag{18}$$

A comparison with (1) leads to

$$\sqrt{\left(\frac{\bar{\tau}_W}{\rho}\right)} = \bar{U} \sqrt{\left(\frac{\lambda}{8}\right)}. \tag{19}$$

Correspondingly, equation (19) yields for the respective zones:

$$\sqrt{\left(\frac{\tau_{W1}}{\rho}\right)} = \bar{U}_1 \sqrt{\left(\frac{\lambda_1}{8}\right)} \tag{20}$$

$$\sqrt{\left(\frac{\tau_{W2}}{\rho}\right)} = \bar{U}_2 \sqrt{\left(\frac{\lambda_2}{8}\right)}. \quad (21)$$

The condition that the pressure drop in both zones is equal to that in the entire channel (18) results in

$$\frac{\bar{\tau}_W}{D} = \frac{\tau_{W1}}{D_1} = \frac{\tau_{W2}}{D_2} \quad (22)$$

hence,

$$\frac{\tau_{W1}}{\bar{\tau}_W} = \frac{D_1}{D} \quad \frac{\tau_{W2}}{\bar{\tau}_W} = \frac{D_2}{D} \quad \frac{\tau_{W1}}{\tau_{W2}} = \frac{D_1}{D_2}. \quad (23)$$

Substitution of the respective areas and perimeters according to Fig. 1 and the use of equations (3)–(5) finally yields:

$$\frac{\tau_{W1}}{\bar{\tau}_W} = \frac{\beta^2 - \alpha^2}{\alpha(1-\alpha)} \quad \frac{\tau_{W2}}{\bar{\tau}_W} = \frac{1-\beta^2}{1-\alpha}$$

$$\frac{\tau_{W1}}{\tau_{W2}} = \frac{\beta^2 - \alpha^2}{\alpha(1-\beta^2)}. \quad (24)$$

Extension with $D = 2(r_2 - r_1)$ and $\bar{\tau}_W$ of equation (16) yields:

$$\frac{\tau_{W1}}{\tau_{W2}} = \frac{2{\cdot}5 \ln\left[\frac{r_2 - r_0}{\nu} \cdot \frac{D}{2(r_2 - r_1)} \sqrt{\left(\frac{\tau_{W2}}{\bar{\tau}_W}\right)} \sqrt{\left(\frac{\bar{\tau}_W}{\rho}\right)}\right] + 5{\cdot}5}{2{\cdot}5 \ln\left[\frac{r_0 - r_1}{h}\right] + R(h^+)} \quad (25)$$

Under the logarithm in the numerator the quantity $\bar{\tau}_W/\rho$ can be replaced by $\bar{U}^2\lambda/8$ of equation (19); it appears that

$$\frac{D \cdot \bar{U}}{\nu} = Re. \quad (26)$$

The use of equations (3)–(5) and (24) results in

$$\sqrt{\left(\frac{\beta^2 - \alpha^2}{\alpha(1-\beta^2)}\right)} = \frac{2{\cdot}5 \ln\left[\frac{1-\beta}{2(1-\alpha)} \sqrt{\left(\frac{1-\beta^2}{1-\alpha}\right)} Re \sqrt{\left(\frac{\lambda}{8}\right)}\right] + 5{\cdot}5}{2{\cdot}5 \ln\left[\frac{\beta - \alpha}{\alpha \frac{h}{r_1}}\right] + R(h^+)}. \quad (27)$$

Correspondingly, equations (10) and (11) are transformed:

$$\sqrt{\left(\frac{8}{\lambda_1}\right)} = 2{\cdot}5 \ln\left[\frac{\beta - \alpha}{\alpha \frac{h}{r_1}}\right] + R(h^+) - G_1(\gamma) \quad (28)$$

$$\sqrt{\left(\frac{8}{\lambda_2}\right)} = 2{\cdot}5 \ln\left[\frac{1-\beta}{2(1-\alpha)} \sqrt{\left(\frac{1-\beta^2}{1-\alpha}\right)} Re \sqrt{\left(\frac{\lambda}{8}\right)}\right] + 5{\cdot}5 - G_2(\beta). \quad (29)$$

Equations (19)–(21) and the respective area ratios, change equation (17) into

$$\sqrt{\left(\frac{\lambda}{\lambda_1}\right)} \frac{\beta^2 - \alpha^2}{1 - \alpha^2} \sqrt{\left(\frac{\beta^2 - \alpha^2}{\alpha(1-\alpha)}\right)} + \sqrt{\left(\frac{\lambda}{\lambda_2}\right)} \frac{1-\beta^2}{1-\alpha^2} \sqrt{\left(\frac{1-\beta^2}{1-\alpha}\right)} = 1. \quad (30)$$

Equations (27)–(30) as well as (12) and (13) provide a means of interpretation with α, Re, λ, h/r_1 being given and $\beta(\tau = 0)$, λ_1, λ_2 and $R(h^+)$ as well as h^+ being calculated. Besides, the equations can be used for calculation of the pressure loss (λ) if α, Re, h/r_1 (height of roughness elements) and $R(h^+)$ (form of roughness elements) are known.

RESULTS OF INTERPRETATIONS OF ANNULAR GAP MEASUREMENTS

The following results are restricted to measurements performed with transversal fins of rectangular profile as shown in Fig. 3. Feurstein and Rampf [2] indicate measured results obtained from these roughnesses in diagrams in which λ is plotted over Re. The method of interpretation is demonstrated first by an example. In a diagram which shows the

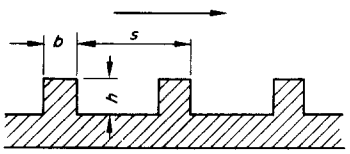

FIG. 3. Shape of roughness elements.

measured results for a specific form and height of roughness the λ-values related to several Reynolds numbers are read and interpreted with the help of the equations indicated above. The result is shown in Table 1.

Table 1. Interpretation; measured values derived from ([2] Fig. 14), Rectangular roughness s/h = 5; h/b = 1·67

$10^{-4}Re^*$	λ^*	β	h^+	$R(h^+)$
2	0·072	0·8694	86·8	3·45
3	0·0665	0·8725	125·8	3·69
5	0·0622	0·8785	204·9	3·82
7	0·0604	0·8833	285·1	3·83
10	0·0595	0·8891	408·3	3·77
20	0·058	0·8995	820·5	3·67

For all values: $\alpha = 0{\cdot}5197$; $h/r_1 = 0{\cdot}6061$.
* measured values taken from [2], Fig. 14.

Table 2. Determination of roughness constants R

$h^*_{(mm)}$	λ^*	h^+	s/h	h/b*	R
	0·0295	374·7	$1{\cdot}1\overline{6}$		10·6
	0·0316	395·7	$1{\cdot}6\overline{6}$		9·78
3	0·048	533·1	2·5	2·5	6·12
	0·059	609·2	$3{\cdot}3\overline{3}$		4·84
	0·08	734·2	$6{\cdot}6\overline{6}$		3·33
	0·028	239·4	1·75		10·25
	0·036	290·9	2·5		7·43
2	0·05	365·1	3·75	$1{\cdot}6\overline{6}$	4·83
	0·0595	408·3	5		3·77
	0·063	423·2	10		3·46
	0·059	406·1	15		3·82
	0·0314	131·2	3·5		7·12
	0·0398	156·4	5		4·8
1	0·0482	178·2	10	$0{\cdot}83\overline{3}$	3·35
	0·0413	160·5	20		4·5
	0·035	142·5	30		5·97
	0·0318	66·3	7		5·23
	0·0392	77·3	10		3·2
0·5	0·0343	70·2	20	$0{\cdot}41\overline{6}$	4·43
	0·028	59·9	40		6·78
	0·0252	54·7	60		8·31

* = measured values derived from [2].
$\alpha = 0{\cdot}5197$; $Re = 10^5$.

It appears that the $\tau = 0$ line moves towards the outer wall with increasing Reynolds number; the quantity $R(h^+)$ first increases and then reaches an almost constant level.

I now assume that for all forms of roughness investigated by Feurstein and Rampf [2] a constant value of $R(h^+)$ is obtained for high values of h^+ and calculate this value from the measurements at $Re = 100000$. The result of the interpretation with respect to 21 measured forms of roughness is shown in Table 2.

On the basis of these results and using additional measured values, it will be attempted in the following paragraphs to indicate for this form of roughness—transversal ribs and rectangular profile—the dependence of the quantity R on the parameters s/h and h/b, which characterize this type of roughness.

COMPARISON OF MEASURED RESULTS ON TRANSVERSAL RIBS

Quite a number of measured results are indicated in the literature which were obtained on transversal fins with rectangular profiles. The flow channels investigated were circular tubes, parallel plates and annular gaps. The experimental techniques employed included either measurements of the velocity profile and, hence, the direct determination of $R(h^+)$, or measurements of the pressure loss and determination of $R(h^+)$ by the method of interpretation described above. The measured values were discussed in [1] and have been summarized in Table 3. The first 12 results which are given by Kjellström and Hedberg [4], Hewitt [5], Hewitt and Kearsey [6], and Kaul and V. Kiss [7] and were derived from pressure loss measurements carried out on annular gaps. Pressure loss measurements made on circular tubes resulted in values by Nunner [8], Koch [9] and Sams [10]. Finally, the measured values by Schlichting [11] are indicated which are velocity measurements performed on parallel plates.

Figure 4 indicates the results obtained on a

total of 48 test sections (Tables 2 and 3). Empirical curves are plotted the parameters of which represent the relative rib width. The influence of rib width is particularly great in case of small distance ratios. Consequently, the geometrical shape of the rib plays a decisive part. This implies for the experiments that the ribs must be fabricated with utmost care to ensure geometrical similarity. It is supposed that the scattering of measured points in Fig. 4 can be explained partly by such geometrical discrepancies. For each rib width, R is a minimum at a defined distance ratio; however, it seems that it never becomes less than approximately 2·5.

Table 3. Parameters pertaining to Fig. 4

s/h	h/b	R	Lit.
1·85	4	7·33	[3]
3·95	1·818	3·08	
8·2	1	3·03	
15·6	0·526	4·08	
18·8	0·4348	4·72	
10·7	0·769	3·18	
23·4	0·345	6·97	
27·5	0·303	5·97	
23·5	0·0862	6·44	
17·6	0·2564	6·49	
27·8	1	6·08	
7·9	0·345	7·38	
8·92	0·92	2·04	[4]
16·9	0·8	4·92	[5]
8·33	0·6	3·04	
10	2	2·38	[6]
15	1	3·54	
10	1	3·21	[7]
20·4	0·8	4·45	[8]
3·92	5	3·47	[9]
9·8	5	3·16	
1·46	1·37	7·42	
2·056	0·862	9·33	[10]
2·274	0·88	12·12	
18·75	10·7	4·17	
12·9	10·3	2·28	[11]
6·67	10	2·33	

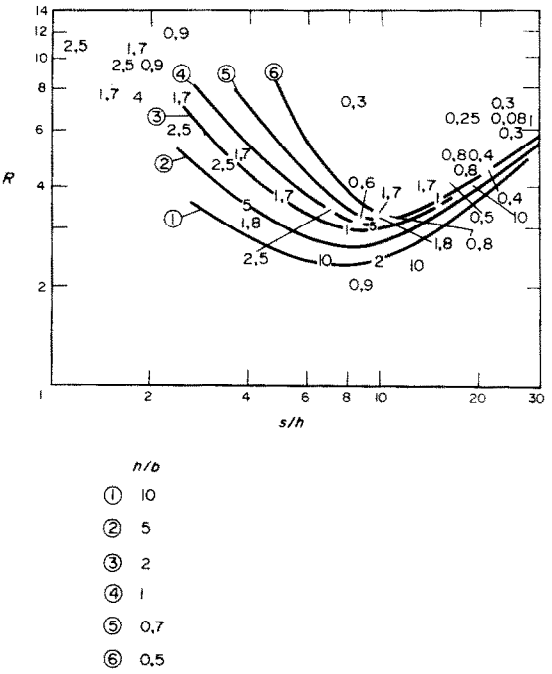

FIG. 4. Roughness Parameter—rectangular ribs.
Results of measurements are given with the corresponding value of h/b.

CALCULATION OF FRICTION FACTORS IN A ROUGH ANNULAR GAP WITH TRANSVERSAL RIBS

For calculation of the friction factors of turbulent flow in annular gaps with roughened inner tube equations (27)–(30), (12) and (13) are properly evaluated. First, the calculated friction coefficients will be compared with the values measured by Feurstein and Rampf [2].

Figures 5 and 6 show the results. The given values of s/h and h/b allow to take R from Fig. 4 and λ was calculated for the respective values of α and h/r_1 for different Reynolds numbers. From [2], (Figs. 12–15), the respective measured values of λ were read for $Re = 2 \times 10^4, 5 \times 10^4, 10^5, 2 \times 10^5$ and entered as points. Deviations are less than 10 per cent.

Figure 7 shows a comparison of friction factors with once the Nikuradse sand roughness

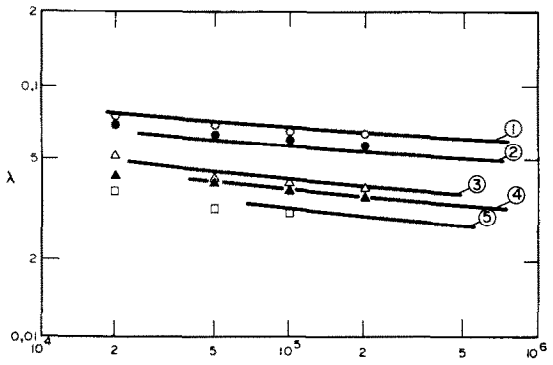

	s/h	h/b	R	h/r₁	[2], Bild Nr.	Measured
①	10	1,66	3,1	0,0606	14	○
②	5	1,66	4,05	0,0606	14	●
③	20	0,83	4,3	0,0303	13	△
④	10	0,41	3,4	0,0515	12	▲
⑤	5	0,41	5,0	0,0515	12	□

FIG. 5. Comparison of calculated with measured friction factors of [2]. Annulus = 0·5197.

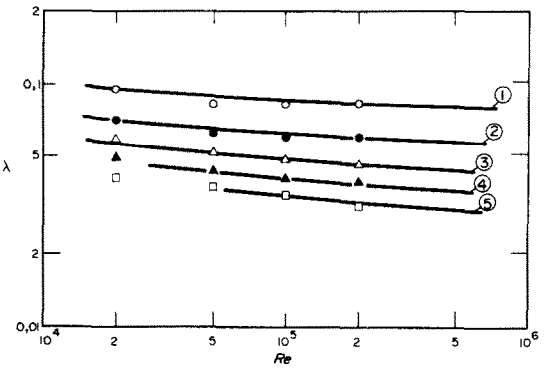

	s/h	h/b	R	h/r₁	[2], Bild Nr.	Measured
①	6,66	2,5	3,1	0,0909	15	○
②	15	1,66	3,6	0,0606	14	●
③	10	0,83	3,2	0,0303	13	△
④	5	0,83	4,75	0,0303	12	▲
⑤	20	0,41	4,3	0,0515	12	□

FIG. 6. Comparison of calculated with measured friction factors of [2]. Annulus = 0·5197.

and then a transversal rib with an $R = 2{\cdot}6$ applied to the central tube. $R = 2{\cdot}6$ results from Fig. 4 for a rectangular rib with $s/h = 8$ and $h/b = 5$. It appears that with $Re = 10^5$ and $h/r_1 = 0{\cdot}1$ the friction factor is about a factor of 2·7 higher for the transversal rib than in the case of identically high sand roughness.

Figure 8 shows the rate of increase of the

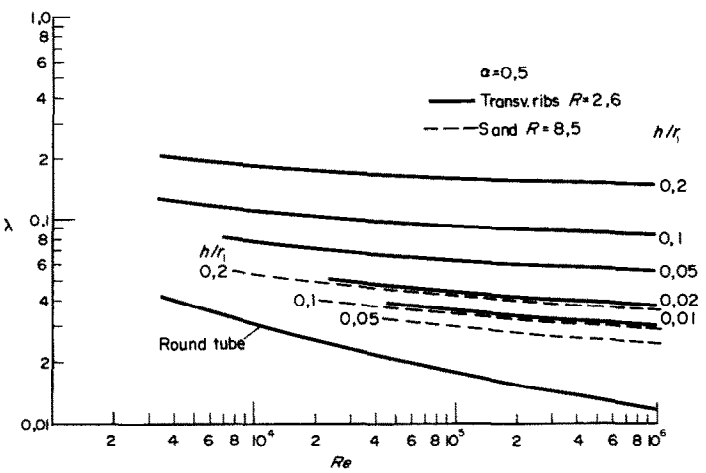

FIG. 7. Comparison sand-roughness– transversal ribs.

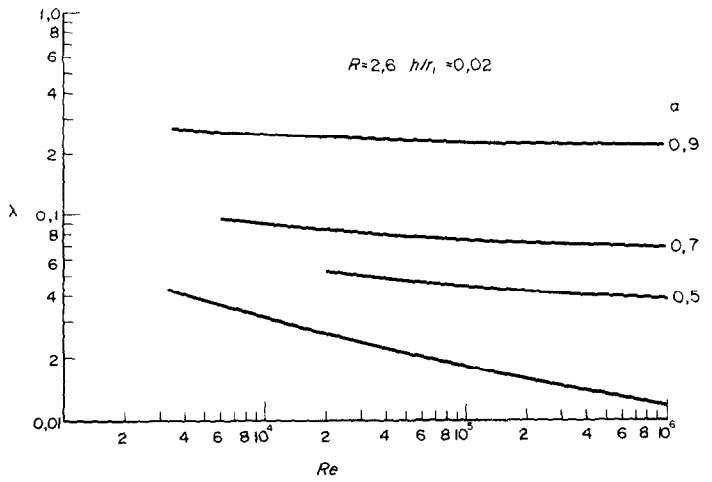

FIG. 8. Influence of r_1/r_2 on friction factor.

friction factor with increasing α and reduction, respectively, of the gap between the central and the outer tube.

Finally, Fig. 9 shows an example in which way the friction factor of the entire channel is generated from the friction factors of the two zones. The typical development in the smooth outer zone is clearly visible. In the inner zone R is constant, but not the friction factor, since β varies, i.e. the location of the $\tau = 0$ line moves to the outside with Re. Related points are marked by identical symbols.

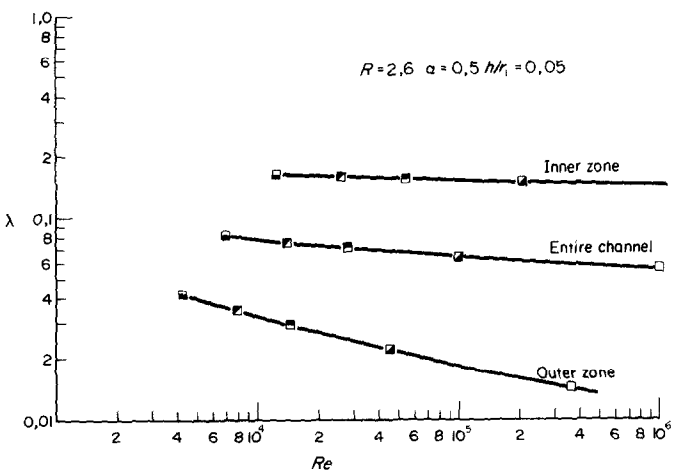

FIG. 9. Friction factors, inner zone, outer zone, total channel.

SUMMARY

Calculation of the pressure loss of turbulent flows in annular gaps with wall roughnesses requires knowledge of the parameters which determine the effect of roughness on the velocity profile. The equations are indicated which describe the isothermal turbulent flow in concentric annular gaps with roughened inner tubes. These equations are used to determine the parameter of the rough velocity profile $R(h^+)$ from measurements of the pressure drop only. With respect to transversal ribs with rectangular profile this parameter is obtained from numerous measurements performed by different authors and a diagram is presented which shows $R(h^+)$ in the interesting range characterized by the distance ratio s/h and the width ratio h/b.

The equations are used also to calculate the pressure drop for a given channel geometry (ratio of diameters), the flow velocity (Reynolds number), and the form and height of roughness, with $R(h^+)$ read from the diagram mentioned. The comparison of calculated friction factors with the measured results provides good agreement. Examples are given to demonstrate the influence exerted on the friction factor by different forms of roughness and heights as well as the ratio of diameters.

The results show that the method described can be used to calculate the pressure loss of turbulent flows in concentric rough annular gaps with an accuracy sufficient for technical application.

REFERENCES

1. K. MAUBACH, Reibungsgesetze turbulenter Strömungen *Chemie-Ingenieur-Technik* **42** (15), 995–1004 (1970).
2. G. FEURSTEIN und H. RAMPF, Der Einfluss rechteckiger Rauhigkeiten auf den Wärmeübergang und den Druckabfall in turbulenter Ringspaltströmung. *Wärme- und Stoffübertragung* **2**(1), 19–26 (1969).
3. B. KJELLSTRÖM and A. E. LARSSON, Improvement of reactor fuel element heat transfer by surface roughness. Report AE-271. Atomeuergie AB, Studsvik, Sweden (1967).
4. B. KJELLSTRÖM and S. HEDBERG, On shear stress distribution for flow in smooth or partially rough annuli. EAES Heat Transfer Symp., Bern (August 1966), Report AE-243 (1966).
5. G. F. HEWITT, Interpretation of pressure drop data from an annular channel, AERE-R 4340 (1964).
6. G. F. HEWITT and H. A. KEARSEY, Heat transfer to superheated steam from roughened surfaces. EAES Heat Transfer Symp., on superheated steam or gas, Bern (August 1966).
7. V. KAUL and M. VON KISS, Forced convection heat transfer and pressure drop in artificially roughened flow passages, *Neue Technik* **6**, 297 (1964).
8. W. NUNNER, Wärmeübergang und Druckabfall in rauhen Rohren, *VDI-Forsch. Heft* 455 Düsseldorf (1956).
9. R. KOCH, Druckverlust und Wärmeübergang bei verwirbelter Strömung, *VDI-Forsch. Heft* 469 Düsseldorf (1958).
10. E. W. SAMS, Experimental investigation of average heat transfer and friction coefficients for air, NACA-RM-E52D17.
11. H. SCHLICHTING, Experimentelle Untersuchungen zum Rauhigkeitsproblem, *Ing. Archiv* **7**(1), 1–34 (1936).

CHUTE DE PRESSION POUR ESPACE ANNULAIRE RUGUEUX. INTERPRETATION DES EXPERIENCES ET CALCUL POUR DES STRIES CARREES

Résumé—On présente une méthode qui permet l'interprétation des mesures de chute de pression dans les tubes rugueux, les espaces annulaires et les plans parallèles. Un paramètre décrit l'effet de la rugosité sur un profil de vitesse turbulente. En conséquence les mesures expérimentales avec différentes rugosités et géométries de conduit peuvent être généralisées et rendues comparables. Le mémoire résume les résultats de l'interprétation des essais avec des rugosités à section droite rectangulaire donnés par plusieurs auteurs dans la bibliographie.

On donne enfin des exemples de calcul de coefficient de frottement pour des nombres de Reynolds, des géométries de conduit et de rugosité données. Ces résultats prouvent que la méthode proposée permet de calculer les coefficients de frottement pour un écoulement turbulent isotherme dans un espace annulaire à tube intérieur rugueux avec une précision qui est suffisante pour les projets.

DRUCKVERLUST IN RAUHEN RINGSPALTEN. INTERPRETATION VON EXPERIMENTEN UND BERECHNUNG FÜR RECHTECKIGE QUERRIPPEN

Zusammenfassung – In dieser Arbeit wird eine Methode zur Interpretation von Druckverlustmessungen an rauhen Rohren, Ringspalten und parallelen Platten dargestellt, wobei ein Parameter angegeben wird, der die Wirkung der Rauhigkeitselemente auf das turbulente Geschwindigkeitsprofil beschreibt. Damit wird es möglich, Messwerte, die an verschiedenen Rauhigkeitsformen und Kanalgeometrien gewonnen werden, zu verallgemeinern und zu vergleichen. Die Messergebnisse vieler Autoren an Rauhigkeiten mit Rechteckquerschnitt werden auf diese Weise interpretiert und zusammengestellt angegeben.

An einigen Beispielen wird schliesslich die Berechnung des Reibungsbeiwertes gezeigt; dabei werden die Reynolds-Zahl der Strömung, die Kanal- und Rauhigkeitsform vorgegeben.

Die Ergebnisse zeigen, dass die beschriebene Methode es erlaubt, die Reibungsbeiwerte der isothermen turbulenten Strömung in konzentrischen Ringspalten mit rauhem Innenrohr mit, für Auslegungsprobleme ausreichender Genauigkeit zu berechnen.

ПЕРЕПАД ДАВЛЕНИЯ В ШЕРОХОВАТОМ КОЛЬЦЕВОМ КАНАЛЕ. ОБРАБОТКА ЭКСПЕРИМЕНТАЛЬНЫХ ДАННЫХ И ПЕРЕСЧЁТ ДЛЯ ПРЯМОУГОЛЬНЫХ РЁБЕР

Аннотация—Описан метод, позволяющий обработать измеренные значения перепада давления для шероховатых труб, кольцевых каналов и параллельных пластин. Выведенный параметр описывает влияние шероховатости на профиль турбулентной скорости. В результате экспериментальные данные по различным шероховатостям и геометриям канала можно обобщить и привести к сопоставимому виду. В статье суммируются результаты обработки данных для элементов шероховатостей прямоугольного сечения, приведенных в литературе многочисленными авторами.

Наконец, приводятся примеры пересчета коэффициентов трения при условии заданных значений критерия Рейнольдса в канале и геометрий шероховатости. Результаты подтверждают, что предложенный метод позволяет рассчитать коэффициенты трения для изотермического турбулентного течения в концентрических кольцевых каналах с шероховатыми внутренними стенками с точностью, достаточной для инженерных расчетов.